ELSEVIER

Chemical Engineering Science 61 (2006) 8040–8049

Chemical Engineering Science

www.elsevier.com/locate/ces

Laser-based planar imaging of nano-particle fluidization: Part II—mechanistic analysis of nanoparticle aggregation

X.S. Wang[a], V. Palero[b], J. Soria[c], M.J. Rhodes[a,*]

[a]*Department of Chemical Engineering, Monash University, P.O. Box 36, Clayton 3800, Australia*
[b]*Department of Applied Physics, I3A-Universidad de Zaragoza, 50009 Zaragoza, Spain*
[c]*Laboratory for Turbulence Research in Aerospace & Combustion, Monash University, Clayton Campus, VIC 3800, Australia*

Received 13 June 2006; received in revised form 26 September 2006; accepted 26 September 2006
Available online 1 October 2006

Abstract

Degussa Aerosil R974 powder, with a primary particle size of 12 nm, was fluidized using nitrogen in a glass vessel of 46 mm square cross-section. Images of nanoparticle aggregates were recorded with a high-resolution digital CCD camera. The settling velocities of the nanoparticle aggregates were obtained through PIV (particle image velocimetry) analysis and manual tracking of individual aggregates. The results enabled an assessment of the applicability of the Richardson–Zaki equation to nanoparticle fluidization. The internal structure and formation mechanisms of nanoparticle aggregates formed under fluidization conditions are discussed in the light of the results obtained.

Keywords: Aerosol; Agglomeration; Fluidization; Nanoparticle; Particle processing; PIV

1. Introduction

Nanoparticle fluidization has been a topic of increasing research interest over recent years due to its potential applications in reaction engineering, particle formation, processing and coating. It is now commonly accepted that nanoparticles may be fluidized in the form of "light" and "loose" aggregates, and that the fluidized suspension of nanoparticles is "fluid-like". In addition, there appears to be a consensus among researchers that bed expansion of nanoparticles may be described by the well-known Richardson–Zaki (R–Z) equation, i.e. $U/U_t = \varepsilon^n$, where U is superficial gas velocity, U_t is terminal velocity of a single aggregate, ε is the voidage surrounding the aggregates, and n is a constant. However, there exists a degree of empiricism and confusion concerning how the value of ε may be determined. In the work of Wang et al. (2002), the value of ε was taken to equal the overall bed voidage, assuming that the density of the aggregates were the same as that of the expanded (fluidized) bed. Zhu et al. (2005) argued that the voidage for the R–Z equation should be differentiated from the overall bed voidage. They estimated the value of ε by assuming that the density of the aggregates remained constant before and during fluidization.

Valverde and Castellanos (2006) proposed a modified R–Z equation for describing nanoparticle fluidization. The analysis of Valverde and Castellanos was based on concepts of "simple" and "complex" structures, which have an origin in an earlier paper by Wang et al. (2002). There are doubts whether the aggregates obtained by Wang et al. (2002) truly represent those under fluidization conditions. First, the samples could be increasingly consolidated if they were left inside the bed for too long. Second, in the process of getting the samples out of the bed, the samples could be contaminated by particles resting near the sampling ports. Third, for TEM imaging, the samples had to undergo treatment (e.g., with a solution), which could alter the original structure of the aggregates. Valverde and Castellanos assumed that "simple" agglomerates are present in the as-received powder while "complex" agglomerates are formed by a dynamic equilibrium process in the fluidized bed. These assumptions are yet to be rigorously tested.

On the other hand, many authors refer to the R–Z equation when they really mean that a linear relationship exists between $\log(\varepsilon)$ and $\log(U)$. Analysis shows that the above linear

* Corresponding author. Tel.: +61 3 9905 3445; fax: +61 3 9905 5686.
E-mail address: martin.rhodes@eng.monash.edu.au (M.J. Rhodes).

0009-2509/$ - see front matter © 2006 Elsevier Ltd. All rights reserved.
doi:10.1016/j.ces.2006.09.046

relationship indeed leads to an expression remarkably similar to the R–Z equation, i.e., $U/U' = \varepsilon^n$, where n is the gradient of the straight line on the $\log(\varepsilon)$ versus $\log(U)$ plot. But there is no guarantee that the value of U' in the above expression equals the terminal velocity of a single aggregate. Unfortunately, no measurements of the terminal velocities of individual nanoparticle aggregates can be found in the open literature. In addition, our current knowledge of the properties of nanoparticle aggregates does not permit calculation of terminal velocities of the aggregates with confidence.

Advances in understanding the mechanisms of nanoparticle aggregation have been propelled by computer simulations. For detailed information of the computational techniques and algorithms applied in these simulations, the reader should refer the book edited by Stanley and Ostrowsky (1986). A description of the key mechanisms, which include diffusion-limited aggregation (DLA), ballistic aggregation, and reaction-limited aggregation, can be found in Friedlander (2000). Despite some recent success in characterization of nanoparticle aggregates (e.g., Wang et al., 2006), our knowledge of the internal structure and formation mechanisms for the nanoparticle aggregates is still far from satisfactory. In this paper, we present laser-based planar imaging measurements of the settling velocities of nanoparticle aggregates formed under fluidization conditions. The usefulness of the results for understanding the mechanisms of nanoparticle aggregation is demonstrated.

2. Experimental apparatus and methodology

2.1. Fluidized bed facility

The fluidized bed used in this study is shown schematically in Fig. 1. The fluidization vessel was constructed from 6-mm-thick flat glass plates, which were glued together by UV adhesive (LOCTITE® 358). The inside dimensions of the fluidization vessel were 46 mm × 46 mm in cross section and 800 mm high. High-purity nitrogen was supplied to the bed through a porous distributor plate, 3 mm thick, made from sintered bronze with a nominal pore size of 10 μm. The flow rate of nitrogen was controlled by a needle valve and measured with a rotameter. The particles used were Aerosil R974 (Degussa) hydrophobic silica. The primary particle size and particle density of the powder were 12 nm and 2200 kg/m^3, respectively, with a bulk density of 30 kg/m^3 and external surface area of 200 m^2/g. The pressure drop through the bed was measured with a digital manometer. Before being vented to the atmosphere, the exhaust gas was filtered using a porous metal filter with 5 μm nominal pore size, and further cleaned by water scrubbing. The pressure drop through the porous metal filter was monitored using a normal water-manometer. The metal filter was cleaned using reversed pulsed flow of nitrogen before each experiment.

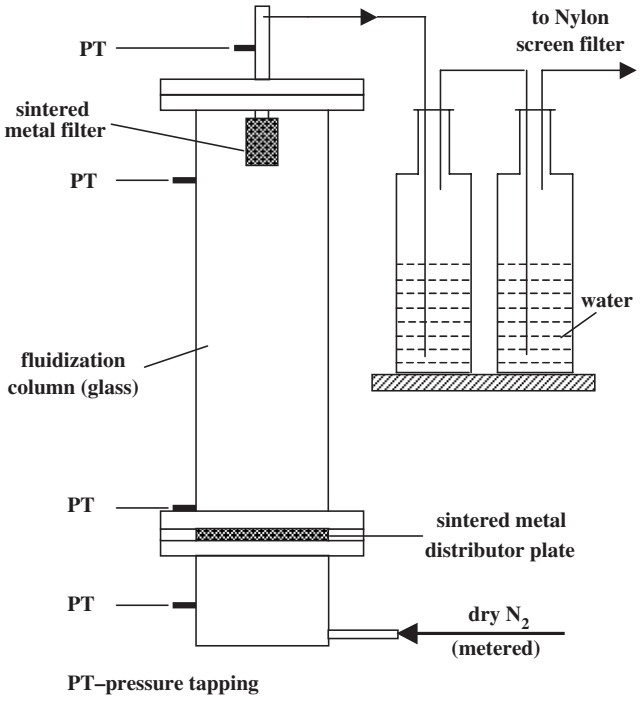

Fig. 1. Schematic diagram of experimental set-up.

2.2. Laser-based planar imaging of nanoparticle fluidization

Particle image velocimetry (PIV) is a quantitative flow structure visualization technique enabling measurement of the instantaneous in-plane velocity vector field within a planar section of the flow field (Soria, 1996). In a typical PIV experiment a plane of a fluid is illuminated with a laser sheet. Previously the fluid is seeded with small particles (typically in the range of 1–10 μm) of the same density as the fluid. These particles act like tracers, scattering light and following the path of the fluid flow. The image of the particles in the illuminated plane is recorded with a CCD camera whose optical axis is perpendicular to the fluid plane. In order to obtain the flow velocity two consecutive images are recorded with a known time interval (Δt) between them. The particle displacement on each point of the fluid plane is obtained by dividing the images in small interrogation areas (IA) and calculating the cross-correlation function between the same IA in both images. The local velocity is calculated by dividing the measured local displacement by Δt after having taken the optical magnification into account.

A schematic of our PIV system is shown in Fig. 2. The symbols used for describing the optical system are explained in the "Notation" section. Two Nd:YAG pulsed lasers ($\lambda = 532$ nm, 100 mJ per pulse, 5 ns pulse width) were used to record the image pairs. The lasers were overlapped through a beam splitter plate and shaped into a sheet to illuminate a plane within the fluidized bed. Two cylindrical lenses ($f1 = -60$ mm, $f2 = 200$ mm) formed the laser sheet. A telecentric lens ($f = 55$ mm, $f\# = 2.8$) was used to image the illuminated plane onto the CCD sensor of a digital camera. The CCD array contained 1280 pixels × 1024 pixels each having a nominal size of 6.7 μm × 6.7 μm. The optical magnification was set at 0.216. The lasers and the camera were synchronized with a real-time linux computer program that allowed the control of the time interval between the two consecutive